Prioritizing TESS Planet Candidates

Balancing Earth-Likeness and HST Resource Requirements

The Transiting Exoplanet Survey Satellite (TESS) has so far discovered a multitude of potentially habitable planet candidates. The next step in confirming the habitability of these exoplanets will be spectroscopic observations to determine mass and composition. In an effort to prioritize candidates for these observations, we propose to use an Earth Similarity Confidence Metric (ESCM) calculated using probability density functions for the Earth Similarity Indexes (ESIs; Schulze-Makuch, D. et al., 2011) of TESS planet candidates (TPCs). This metric will be weighed against the exposure time required to complete a particular observation in a benefit:cost ratio with the resultant values given equivalent prioritization. This simple ratio is a flexible and robust method to prioritize observations of TPCs intended to detect and confirm the habitability of exoplanets.

The specific definitions of what constitutes a generally habitable planet are inextricably linked to life as we know it, i.e. life on Earth. Thus, as we understand habitability, the search for habitable exoplanets is a search for relatively Earth-like worlds. In order to characterize exoplanets in this way, we propose to use the global Earth Similarity Index (ESI) as described in Schulze-Makuch et al. (2011). Though this method is relatively simple, it works especially well for the limited data available on observed exoplanets. In addition, its flexible nature lends itself well to use in prioritization as the values used in its calculation and the weights given to the ESIs can easily be changed depending on the requirements and goals of a particular observation.

Due to the lack of observations and types of observations conducted on the more Earth-like TPCs, we propose to use the global ESI presented in its originating paper (Schulze-Makuch et al., 2011) which is a function of planet radius, density, surface temperature, and surface escape velocity. The global ESI can be calculated as the geometric mean of the ESI of each input variable. These individual ESIs are calculated with the following formula:

$$ESI_x = \left(1 - \left|\frac{x - x_0}{x + x_0}\right|\right)^w$$

where x is the variable, x_0 is that variable's value for the Earth, and w is a weight. Prior to radial-velocity measurements, the mass of TPCs must be inferred. For our initial survey of TPCs, we used the mass-radius relationship proposed by Ning, B. et al. (2018) which is a flexible method based on Kepler observations. Other parameterizations use the same method for calculating the global ESI.

The often non-Gaussian nature and significance of TESS data uncertainties are not accurately represented in this one index. Therefore, we propose to use an ESCM instead that is derived from the ESI calculations. To start, a Monte-Carlo Method is used to construct a probability distribution function (PDF) for the ESI, visually represented in **Figure 1**. In this way,

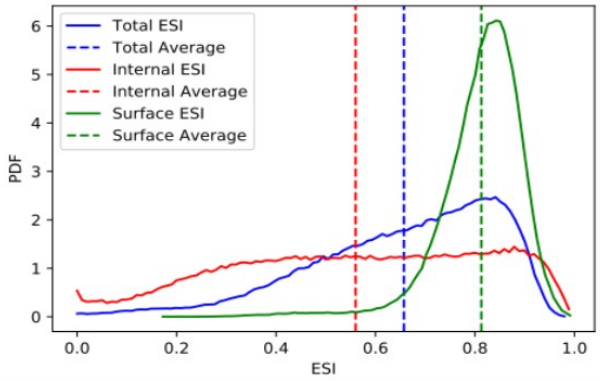

Figure 1. *The internal ESI includes the radius and density ESIs, the surface ESI relates to surface temperature and escape velocity, and the total ESI is the geometric mean of the two. The PDFs of all three ESIs are shown on the graph along with their averages.*

all of the data features and uncertainties can be expressed and taken into account. Then, the PDF is integrated from 0.8 to 1, which corresponds to values that are 'Earth-like,' to calculate the ESCM. This final metric can then be divided by the exposure time required to complete a particular observation of the planet to prioritize the candidate for observation

For an example of the proposed prioritization scheme, consider first the observations of GJ 1214b with the WFC3 instrument by Kriedberg, L. et al. (2014). The data used in their analysis consisted of 16.0593 hours of exposure time, neglecting the unused observations. From a recent survey of TPCs in the habitable zones of their host stars we conducted, TIC ID 201878287, an M-dwarf roughly the same size as GJ 1214, was identified as hosting the most Earth-like TPC with an ESCM of 0.266313. GJ 1214b's ESCM is about 17 times less, whereas the ratio of planet radius to stellar radius is about 3.5 times higher for the GJ 1214 system. As the planet/star radius is the main signal in transit spectroscopy, TIC 201878287 would need around 3.5 times the observation time, but its prioritization would still be 5 times that of GJ 1214b. The ESCMs of 13 TPCs from the first 4 sectors of TESS's observations are given in **Figure 2**. These TPCs are all within their host stars' optimistic habitable zones (Kopparapu, R. et al., 2013) and are of a radius similar to the Earth's, thus representing the most ideal candidates for future observation.

As more data is gathered about these TPCs and more modeling done to simulate the planets once confirmed, this ESCM can be adapted to further prioritize planets for observations even beyond the scope of Hubble. When attempting to characterize a planet's atmosphere based on transit spectroscopy, characteristics relating to the modeled concentrations of observable biomarkers can be used in place of or in conjunction with surface temperature and surface escape velocity. In essence, any parameter of interest during an observation can be added into the ESCM to produce prioritizations. This quality especially makes this relatively simple method useful in planning a wide variety of observations.

Earth Similarity of Select TPCs

TIC ID	Planet Candidate #	Earth Similarity Confidence
270068097	1	0.135192
389527914	1	0.236251
153065527	1	0.127628
37764281	1	0.154546
281573523	2	0.120830
197758148	1	0.160485
259962054	1	0.200162
92350801	1	0.076808
206694354	1	0.107448
152821098	1	0.165261
201878287	1	0.266313
441051650	1	0.202163
38698751	1	0.144284

Figure 2. *This table shows the Earth Similarity Confidences of a selection of potentially Earth-like Planet Candidates.*

References

Kreidberg, L., Bean, J., Désert, J., Benneke, B., Deming, D., Stevenson, K., Seager, S., Berta-Thompson, Z., Seifahrt, A., and Hormeier, D.: Clouds in the Atmosphere of the Super-Earth Exoplanet GJ1214b, Nature, Vol. 505, pp. 69-72, 2014.

Kopparapu, R., Ramirez, R., Kasting, J., Eymet, V., Robinson, T., Mahadevan, S., Terrien, R., Domagall-Goldman, S., Meadows, V., and Deshpande, R.: Habitable Zones Around Main-Sequence Stars: New Estimates, The Astrophysical Journal, Vol. 765, pp. 131-147, 2013.

Ning, B., Wolfgang, A., and Ghosh, S.: Predicting Exoplanets Mass and Radius: A Nonparametric Approach, The Astrophysical Journal, Vol. 869, pp. 5-20, 2018.

Schulze-Makuch, D., Méndez, A., Fairén, A., von Paris, P., Turse, C., Boyer, G., Davila, A., de Sousa António, M., Catling, D., and Irwin, L.: A Two-Tiered Approach to Assessing the Habitability of Exoplanets, Astrobiology, Vol. 11, pp. 1041-1052.

White Dwarf Planetary Systems

Identifying planetesimals with *TESS* and determining their composition with *HST* & *JWST*

Overview

Almost all known planet hosts share a common fate: they will evolve into white dwarfs, the remnants of main-sequence stars with initial masses $\lesssim 8\,M_{\odot}$. Many of the currently known planets will survive the post main-sequence evolution of their host stars – including Mars and the planets beyond in our own Solar System (Schröder & Connon Smith, 2008). The gravitational interactions of these planets can scatter asteroids, moons, and possibly some of the planets themselves deep into the gravitational potential of the white dwarf, where they are tidally disrupted and eventually accreted (Jura, 2003; Veras & Gänsicke, 2015; Payne et al., 2017; Kenyon & Bromley, 2017). Observational evidence for planetary systems at white dwarfs is ample in the form of photospheric contamination of 25 - 50 % of white dwarfs by the accreted debris (Zuckerman et al., 2010; Koester et al., 2014), and dusty (Farihi et al., 2009) and gaseous circumstellar discs (Gänsicke et al., 2006; Manser et al., 2016). Vanderburg et al. (2015) and Manser et al. (2019) established the first photometric and spectroscopic evidence for planetesimals in close orbits around white dwarfs. For recent review papers on evolved planetary systems at white dwarfs, see Jura & Young (2014), Farihi (2016), and Veras (2016).

This white paper describes the capabilities of *TESS* to identify and characterise transiting planetesimals, akin to those found around the white dwarf WD 1145+017 (Vanderburg et al., 2015). Once these systems are identified, follow-up with *HST* spectroscopy is critical to constrain the elemental composition of the planetary body which will provide the input required for a detailed mineralogical study of the debris disc with *JWST* mid-infrared spectroscopy. Fig. 1 schematically illustrates a white dwarf system with a disrupting planetsimal that has formed a debris disc, as well as the synergies arising from combining *TESS*, *HST*, and *JWST* observations.

Identifying transiting planetesimals with *TESS*

The transit features in the lightcurve of WD 1145+017 are generated by clouds of dusty debris originating from several planetesimal fragments orbiting on periods clustered on $\simeq 4.5$ h. Initially discovered in the *Kepler* K2 survey (Vanderburg et al., 2015), the system has attracted a large amount of follow-up observations (Alonso et al., 2016; Xu et al., 2016; Gänsicke et al., 2016), and theoretical studies (Gurri et al., 2017; Veras et al., 2017; Shestakova et al., 2019). Fig. 1 A shows both the complexity of the transiting debris, as well as the significant amount of starlight obscured - up to 50 % at times (Izquierdo et al., 2018).

The detection of a planetesimal orbiting the white dwarf SDSS J1228+1040 (Manser et al., 2019) shows that WD 1145+017 is not a unique system, and we expect that *TESS* will identify additional planetesimals around other white dwarfs. The *TESS* footprint contains $\simeq 1700$ bright white dwarfs ($G_{RP} \lesssim 16$, Gentile Fusillo et al. 2019), the majority of which will have 2 min cadence lightcurves thanks to several approved *TESS* programs to identify white dwarf planetary systems. This sample is larger than the total number of white dwarfs observed with the *Kepler* K2 mission (van Sluijs & Van Eylen, 2018), and the extreme flux changes expected for WD 1145+017-like systems (up to $\simeq 50\%$, Fig. 1 A) could increase the *TESS* sample further using full-frame data.

Transiting planetesimals orbiting close to the tidal disruption radius ($\simeq 1\,R_{\odot}$), will have $\simeq$ hourly periods. Fig. 2 of Vanderburg et al. (2015) demonstrates clearly that the 27 day stare mode of *TESS* and the 2 min cadence are sufficient to detect the transiting planetesimals. Follow-up ground-based observing can easily be obtained on small-aperture telescopes thanks to the deep transits. We

expect that *TESS* will find only a handful of these rare and exciting systems, and obtaining modest follow-up observations will be crucial in understanding their stability and diversity.

The debris discs generated by the disruption of planetesimals, and the subsequent accretion of this material onto white dwarfs provide a unique insight into atomic and mineralogical composition of the parent bodies. However, to capitalise on this, the white dwarf planetary community requires *HST* observations to characterise the elemental composition of these planetesimals in preparation for mid-infrared spectroscopy of dusty discs with *JWST*.

Atomic composition studies with *HST* in the ultraviolet

Fig. 1 C shows a *HST*/COS ultraviolet (UV) spectrum of the white dwarf SDSS J1228+1040, revealing the metal pollution of its otherwise pristine hydrogen atmosphere. Zuckerman et al. (2007) pioneered the spectroscopic analysis of white dwarfs accreting planetary debris to accurately measure the bulk composition of exo-planetary systems, analogous to solar-system meteorite studies. This method has been used to measure the abundances of rock-forming elements (Si, Fe, Mg, O), refractory lithophiles (Ca, Al, Ti), siderophiles (Cr, Mn, Ni), and volatiles (C, N, S, P, most easily detected by *HST*), revealing significant diversity (Gänsicke et al., 2012), which includes evidence for differentiated planetesimals (Wilson et al., 2015; Melis & Dufour, 2017), water-rich exo-asteroids (Farihi et al., 2013; Raddi et al., 2015) and one volatile-rich Kuiper belt-like body (Xu et al., 2017). This work provides important inputs into planet formation models (Carter-Bond et al., 2012; Carter et al., 2015; Harrison et al., 2018).

HST is critical for the compositional study of planetesimals identified by *TESS*. White dwarfs hotter than $\simeq 15,000$ K require UV spectroscopy, as the optical transitions rapidly weaken with increasing temperature (e.g., Fig. 1 of Manser et al. 2016). As *HST* is reaching the end of its life and is the only telescope capable of performing the UV spectroscopy required for white dwarf abundance measurements, it is crucial that any disrupting planetesimals identified by *TESS* are urgently followed up with *HST*. Furthermore, the transient nature of the transits of WD 1145+017 strongly suggests that follow-up of planetesimals detected by *TESS* will be time critical (Rappaport et al., 2018). Observations obtained during the presence of transits will allow unique studies to be performed which include; (i) variations between the UV and optical transits, and (ii) investigation of the circumstellar gas that is generated by disrupting planetesimals (Xu et al., 2016).

Mineralogical studies with *JWST* in the infrared

Only a single debris disc was sufficiently bright to obtain high-quality *Spitzer* infrared spectroscopy. Fig. 1 B shows a mineralogical model dominated by amorphous carbon (now known not to be present from *HST*/COS observations, Xu et al. 2014), amorphous and crystalline silicates, water ice, and metal sulfides to the *Spitzer* spectrum of the circumstellar dust around G 29–38 (Zuckerman & Becklin, 1987; Reach et al., 2005, 2009). Once launched, *JWST* will provide the opportunity to extend such study to $\simeq 40$ known systems, which can all be observed with high signal-to-noise (S/N > 10) in $\lesssim 3$ hours using the LRS module of MIRI, and several can even be observed profitably with its MRS module (e.g., Fig. 9 of Dennihy et al. 2016). It is expected that photometric cross-matches between *Gaia* and infrared surveys such as *WISE* will significantly increase the number of known debris discs (Dennihy et al., 2017; Gentile Fusillo et al., 2019).

Combining far-ultraviolet *HST* and mid-infrared *JWST* spectroscopic observations of dusty white dwarfs will provide bulk chemical compositions at an elemental level from *both* the stellar atmosphere and dust stoichiometry from the disc. This combined information will allow the

formation and evolutionary history of the white dwarf's planetary system to be comprehensively probed (e.g. Bond et al., 2010). Such data will allow the identification of what specific chemical compounds parent bodies were made of, thus enabling detailed physical modelling of the chemical, thermodynamic, and physical history of the accreted material (Mustill et al., 2018).

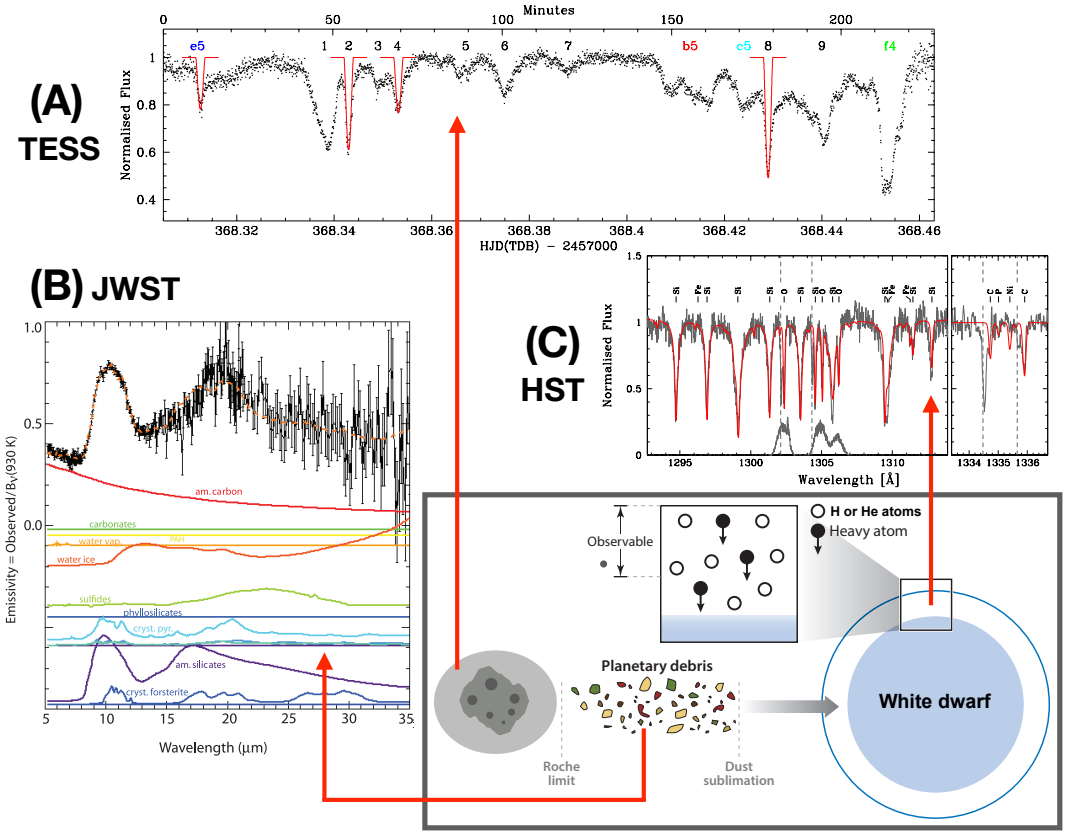

FIGURE 1. *TESS*, *HST*, and *JWST* can be used in conjunction to study exo-planetary bodies and their composition around white dwarfs. **(A)** The transits of multiple disintegrating planetary fragments around WD 1145+017 are complex and block a significant amount of the white dwarf's flux (up to ≃50%, ground-based lightcurve from Gänsicke et al. 2016). The transits were initially discovered using the 30 min cadence observations from the *Kepler* K2 mission (Vanderburg et al., 2015), and *TESS* will be capable of detecting WD 1145+017-like systems within a single 27 day stare. **(B)** *Spitzer*/IRS observations of the debris disc around the white dwarf G 29–38 reveal the mineralogical composition of the disc (reproduced from Reach et al. 2009). *JWST*/MIRI will be able to spectroscopically observe debris discs generated by disrupting planetesimals in a similar way to determine their mineralogical composition. **(C)** The debris disc generated by the disrupting planetesimal will accrete onto the white dwarf and pollute its atmosphere. *HST*/COS observations of UV metal absorption lines can be modelled to determine the atomic composition of the disrupting planetesimal. Figure reproduced from Gänsicke et al. (2012). The schematic of a white dwarf with a planetary debris disc and planetesimal in orbit has been adapted from Jura & Young (2014).

References

Alonso R., Rappaport S., Deeg H. J., Palle E., 2016, A&A, 589, L6
Bond J. C., O'Brien D. P., Lauretta D. S., 2010, ApJ, 715, 1050
Carter-Bond J. C., O'Brien D. P., Delgado Mena E., Israelian G., Santos N. C., González Hernández J. I., 2012, ApJ Lett., 747, L2
Carter P. J., Leinhardt Z. M., Elliott T., Walter M. J., Stewart S. T., 2015, ApJ, 813, 72
Dennihy E., Debes J. H., Dunlap B. H., Dufour P., Teske J. K., Clemens J. C., 2016, ApJ, 831, 31
Dennihy E., Clemens J. C., Debes J. H., Dunlap B. H., Kilkenny D., O'Brien P. C., Fuchs J. T., 2017, , 849, 77
Farihi J., 2016, New Astronomy Reviews, 71, 9
Farihi J., Jura M., Zuckerman B., 2009, ApJ, 694, 805
Farihi J., Gänsicke B. T., Koester D., 2013, MNRAS, 432, 1955
Gänsicke B. T., Marsh T. R., Southworth J., Rebassa-Mansergas A., 2006, Science, 314, 1908
Gänsicke B. T., Koester D., Farihi J., Girven J., Parsons S. G., Breedt E., 2012, MNRAS, 424, 333
Gänsicke B. T., et al., 2016, ApJ Lett., 818, L7
Gentile Fusillo N. P., et al., 2019, MNRAS, 482, 4570
Gurri P., Veras D., Gänsicke B. T., 2017, MNRAS, 464, 321
Harrison J. H. D., Bonsor A., Madhusudhan N., 2018, MNRAS, 479, 3814
Izquierdo P., et al., 2018, MNRAS, 481, 703
Jura M., 2003, ApJ Lett., 584, L91
Jura M., Young E. D., 2014, Annual Review of Earth and Planetary Sciences, 42, 45
Kenyon S. J., Bromley B. C., 2017, , 844, 116
Koester D., Gänsicke B. T., Farihi J., 2014, A&A, 566, A34
Manser C. J., et al., 2016, MNRAS, 455, 4467
Manser C. J., et al., 2019, Science, 364, 66
Melis C., Dufour P., 2017, ApJ, 834, 1
Mustill A. J., Villaver E., Veras D., Gänsicke B. T., Bonsor A., 2018, MNRAS, 476, 3939
Payne M. J., Veras D., Gänsicke B. T., Holman M. J., 2017, MNRAS, 464, 2557
Raddi R., Gänsicke B. T., Koester D., Farihi J., Hermes J. J., Scaringi S., Breedt E., Girven J., 2015, MNRAS, 450, 2083
Rappaport S., Gary B. L., Vanderburg A., Xu S., Pooley D., Mukai K., 2018, MNRAS, 474, 933
Reach W. T., Kuchner M. J., von Hippel T., Burrows A., Mullally F., Kilic M., Winget D. E., 2005, ApJ Lett., 635, L161
Reach W. T., Lisse C., von Hippel T., Mullally F., 2009, ApJ, 693, 697
Schröder K., Connon Smith R., 2008, MNRAS, 386, 155
Shestakova L. I., Demchenko B. I., Serebryanskiy A. V., 2019, , 487, 3935
Vanderburg A., et al., 2015, Nat, 526, 546
Veras D., 2016, Royal Society Open Science, 3, 150571
Veras D., Gänsicke B. T., 2015, MNRAS, 447, 1049
Veras D., Carter P. J., Leinhardt Z. M., Gänsicke B. T., 2017, MNRAS, 465, 1008
Wilson D. J., Gänsicke B. T., Koester D., Toloza O., Pala A. F., Breedt E., Parsons S. G., 2015, MNRAS, 451, 3237
Xu S., Jura M., Koester D., Klein B., Zuckerman B., 2014, ApJ, 783, 79
Xu S., Jura M., Dufour P., Zuckerman B., 2016, ApJ Lett., 816, L22
Xu S., Zuckerman B., Dufour P., Young E. D., Klein B., Jura M., 2017, ApJ Lett., 836, L7
Zuckerman B., Becklin E. E., 1987, Nat, 330, 138
Zuckerman B., Koester D., Melis C., Hansen B. M., Jura M., 2007, ApJ, 671, 872
Zuckerman B., Melis C., Klein B., Koester D., Jura M., 2010, ApJ, 722, 725
van Sluijs L., Van Eylen V., 2018, , 474, 4603

The role of HST and TESS in understanding exoplanet atmospheric evolution

The past ten years have seen the emergence of several features in the observed planetary demographics. Some of these features are believed to be in part the consequence of planet atmospheric escape, which is a process causing atmospheric gas to leave the planet's gravitational well and disperse into space. For example, the lack of highly irradiated Neptune-size planets is believed to be the consequence of the intense, and thus rapid, atmospheric escape to which these planets are subject (e.g., Lecavelier et al. 2007; Davis & Wheatley 2009; Lundkvist et al. 2016; Mazeh et al. 2016; Owen & Lai 2018). Fulton et al. (2017; see also Fulton & Petigura 2018 and van Eylen et al. 2018) showed that the radius distribution of sub-Neptunes is bimodal, giving rise to the so called "evaporation valley". Owen & Wu (2017) and Jin & Mordasini (2018) argued that this is the result of atmospheric escape occurring in the first few hundred Myrs following the dispersal of the proto-planetary disk.

In the presence of strong high-energy (X-ray and EUV [100–912 Å], together XUV; <912 Å) stellar irradiation the upper atmosphere of planets heats up and expands, possibly hydrodynamically (e.g., Lammer et al. 2003; Yelle 2004; Murray-Clay et al. 2009; Koskinen et al. 2013a,b, 2014; Khodachenko et al. 2017). High mass loss can be reached in particular when planets are young and their host stars are active (e.g., Skumanich 1972; Pallavicini et al. 1981; Pizzolato et al 2003; Ribas et al. 2005; Tu et al. 2015; France et al. 2018), or for planets just released from the protoplanetary nebula, in which case the escape is driven by the low planetary gravity and high atmospheric temperature (e.g., Sanz-Forcada et al. 2011; Johnstone et al. 2015; Owen & Wu 2016; Fossati et al. 2017; Kubyshkina et al. 2018).

The mechanism of atmospheric escape, its impact on atmospheric structure and composition, and its role in exoplanet evolution can be most thoroughly studied at ultraviolet (UV; 912–3500 Å) wavelengths. This is because at other wavelengths the optical depth of the upper atmosphere is typically too low. Exceptions are the HI Balmer lines (Jensen et al. 2012; Cauley et al. 2015; Yan & Henning 2018), and the HeI triplet at ≈10833 Å (Seager & Sasselov 2000; Oklopcic & Hirata 2018), which can be detected from the ground. However, the Balmer lines trace gas lying typically below what probed in the UV, hence, e.g., do not constrain the fate of the gas lost by the planet. The HeI triplet, instead, is detectable for exoplanets orbiting close to active stars and preferably of spectral type K (Spake et al. 2018; Nortmann et al. 2018; Salz et al. 2018; Mansfield et al. 2018; Allart et al. 2018; Oklopcic 2019). Therefore, UV observations remain the primary channel for studying upper atmospheres and escape, particularly in presence of planets with CO_2/H_2O-dominated atmospheres. Furthermore, HST is the *only* facility currently capable of collecting the necessary UV observations and JWST will not cover the UV.

Thanks to ground-based facilities, the number of detected hot Jupiters adequate for UV transmission spectroscopy observations with HST has steadily increased. A handful of these planets has been observed by HST at UV wavelengths showing that close-in giant planets host extended, escaping atmospheres and allowed to detect metals (e.g., C, Mg, Fe) in the upper

atmosphere (Vidal-Madjar et al. 2003; Fossati et al. 2010; Haswell et al. 2012; Lecavelier et al. 2012; Ehrenreich et al. 2015; Bourrier et al. 2018). These results inspired several independent groups to develop multidimensional models for studying upper atmospheres and escape (e.g., Yelle 2004; García Muñoz 2007; Schneiter et al. 2007; Murray-Clay et al. 2009; Koskinen et al. 2013a,b; Bourrier et al. 2013; Khodachenko et al. 2017; Carroll-Nellenback et al. 2017; Debrecht et al. 2018; Shaikhislamov et al. 2018). The UV observations and their modelling enable us to infer the structure and composition of upper atmospheres, deduce mass-loss rates, unveil the fate of the gas lost by the planet, and gather information about the host star's characteristics (e.g., XUV fluxes and stellar wind; see Fossati et al. 2015a, for a review on exoplanet atmospheric escape).

The role of TESS. Over the years, HST has collected UV transmission spectra for about a dozen systems enabling us to study atmospheric escape across part of the parameter space covered by Gyr-old giant planets. However, there are two key classes of planets that are yet to be studied and that provide the most compelling information for understanding atmospheric evolution: 1) mini-Neptunes/super-Earths hosting atmospheres at the verge between being hydrogen-dominated (i.e., primary) and CO_2/H_2O-dominated (i.e., secondary); 2) young (<500 Myr) planets. The former are key to understand the final stages of the evolution of primary atmospheres and the conditions under which secondary atmospheres rise, while the latter would enable us to study escape when it is strongest, and thus when it most matters. *The lack of HST observations of these pivotal targets is primarily caused by a lack of bright, nearby targets, which is where TESS is providing the necessary contribution.*

Twilight of primary and rise of secondary atmospheres. The Kepler satellite has already detected a large number of transiting mini-Neptunes and super-Earths, but none of them orbit stars close/bright enough for UV transit observations, particularly at Lyα wavelengths, which, because of interstellar medium absorption, are possible only for systems closer than 50–100 pc, depending on the line of sight. TESS' whole-sky coverage and focus on detecting small planets orbiting bright, nearby stars makes this the ideal facility for detecting the systems that are urgently needed to gain insight into the fate of primary atmospheres and rise of secondary atmospheres.

The so far best example of TESS contribution towards our understanding of the final stages of the evolution of primary atmospheres is the detection of the transiting super-Earth π Men c (Huang et al. 2018; Gandolfi et al. 2018). This is an $\sim$4.5 $M_\oplus$ and 2 $R_\oplus$ super-Earth on a 6.3 days orbit around a nearby (18.3 pc) and bright ($V = 5.65$ mag) G0 star. Based on its bulk density, π Men c may contain the remnant of a primary atmosphere or large amounts of H_2O and other heavy molecules in its atmosphere; the measured radius implies that the planet lies inside the radius gap and thus that it may be undergoing rapid atmospheric loss resulting in an extended atmosphere. Detecting HI through HST Lyα transit observations would suggest that the planet has not fully lost its primary atmosphere or that H_2O is present in large quantity. Detecting an extended atmosphere dominated by heavier gases such as O or C, by-products of water and CO_2/CH_4 photodissociation, will suggest that the planet has a secondary atmosphere. HST will soon observe two transits of π Men c in the UV focusing exactly on H, C, and O lines (PI: García Muñoz).

Extreme atmospheric escape. Observing escape at its maximum, that is when it most matters for shaping exoplanet demographics, requires collecting UV transit spectra of planets

younger than 500 Myr. However, the nearest star-forming regions are at distances of 100–200 pc. At these distances, the low stellar fluxes at Earth, the circumstellar and interstellar dust, and ISM absorption greatly hinder our ability to carry out transmission spectroscopy of young planets. Therefore, one would have to rely on stars in nearby young moving groups, such as DS Tuc A (Newton et al. 2019). However, young stars show variability on many temporal and spectral scales, particularly at UV wavelengths, complicating measurements and interpretation of transit light curves (Loyd & France 2014). Observing extreme atmospheric escape requires therefore to find appropriate proxies for young close-in planetary systems. Planets with H-dominated atmospheres in close orbit to intermediate-mass main-sequence stars (IMMSSs; 1.3–2.5 $M_\odot$) may be a viable solution.

Because of the larger stellar radii, hence small transit depths, such systems are hard to find from the ground and TESS provides the ideal platform for detecting them. Fossati et al. (2018) concluded that these planets endure mass-loss rates a few orders of magnitude higher than those of planets orbiting Gyr-old late-type stars, at a level similar to what is expected for young close-in planets (Fossati et al. 2019). Furthermore, the escape mechanisms and conditions on planets orbiting IMMSSs are the same as those of young planets (Fossati et al. 2019). The key advantage is that, because of the high UV-to-infrared fluxes of IMMSSs, it is possible to obtain high-quality transmission spectra, particularly at UV wavelengths. Furthermore, the UV radiation of IMMSSs is dominated by the photospheric continuum, enabling the detection of a much larger range of species, and the lack of activity-related variability in IMMSSs greatly simplifies interpretation (Llama & Shkolnik 2015, 2016).

The role of HST in estimating the stellar XUV fluxes driving the escape. The evolution and stability of planetary atmospheres intimately depend on the XUV irradiation to which planets are subject, and hence to the system's age and orbital separation, and the stellar mass. For example, planets orbiting M dwarfs are particularly prone to atmospheric escape. This is because M dwarfs have a long pre-main-sequence phase characterised by an XUV luminosity that is 10–100 times higher than on the main sequence (e.g., Ribas et al. 2016; Bourrier et al. 2017). It is therefore of pivotal importance to observationally constrain the XUV emission of stars of different spectral types and at different ages.

The stellar EUV radiation is primarily responsible for heating the hydrogen in the upper atmosphere of planets and thus drive escape. However, because of the need to observe from space and of the intervening interstellar medium absorption, the few available EUV spectra are typically of poor quality. To overcome this problem and while waiting for a much needed space telescope with EUV capabilities (e.g., ESCAPE), various teams have developed scaling relations for extrapolating EUV stellar fluxes from UV and/or X-ray observations, which are within reach with the currently available facilities (Sanz-Forcada et al. 2011; Fontenla et al. 2011; Linsky et al. 2014; Chadney et al. 2015; Fossati et al. 2015b; Louden et al. 2017; King et al. 2018; France et al. 2018). Therefore, HST UV transmission spectroscopy observations also enable one constraining the stellar emission powering escape. Finally, increasing the number of systems observed at UV wavelengths will enable a better understanding of how the XUV emission scales with stellar parameters, particularly mass and age.

We recommend focusing UV HST transit observations on sub-Neptunes/super-Earths and on close-in planets to intermediate-mass main-sequence stars.

References:

Allart et al. 2018, Science, 362, 1384; Bourrier et al. 2013, A&A, 551, A63; Bourrier et al. 2017, AJ, 154, 121; Bourrier et al. 2018, A&A, 620, A147; Carroll-Nellenback, et al. 2017, MNRAS, 466, 2458; Cauley et al. 2015ApJ, 810, 13; Chadney et al. 2015, Icarus, 250, 357; Cockell et al. 2016, AsBio, 16, 89; Davis & Wheatley 2009, MNRAS, 396, 1012; Debrecht et al. 2018, MNRAS, 478, 2592; Ehrenreich et al. 2015, Nature, 522, 459; Fontenla et al. 2011, JGRD, 116, 20108; Fossati et al. 2010, ApJL, 714, L222; Fossati et al. 2015a, Astrophysics and Space Science Library, 411, 59; Fossati et al. 2015b, ApJ, 815, 118; Fossati et al. 2017, A&A, 598, A90; Fossati et al. 2018, ApJL, 868, L30; Fossati et al. 2019, ApJ, submitted; France et al. 2018, ApJS, 239, 16; Fulton et al. 2017, AJ, 154, 109; Fulton & Petigura 2018, AJ, 156, 264; Gandolfi et al. 2018, A&A, 619, L10; García Muñoz 2007, P&SS, 55, 1426; Haswell et al. 2012, ApJ, 760, 79; Huang et al. 2018, ApJ, 868, L39; Jensen et al. 2012, ApJ, 751, 86; Jin & Mordasini 2018, ApJ, 853, 163; Johnstone et al. 2015, A&A, 557, A28; Khodachenko et al. 2017, ApJ, 847, 126; King et al. 2018, MNRAS, 478, 1193; Koskinen et al. 2013a, Icarus, 226, 1678; Koskinen et al. 2013b, Icarus, 226, 1695; Koskinen et al. 2014, RSPTA, 37230089; Kubyshkina et al. 2018b, A&A, 619, A151; Lammer et al. 2003, ApJL, 598, L121; Lecavelier et al. 2007, A&A, 461, 1185; Lecavelier et al. 2012, A&A, 543, L4; Linsky et al. 2014, ApJ, 780, 61; Llama & Shkolnik 2015, ApJ, 802, 41; Llama & Shkolnik 2016, ApJ, 817, 81; Louden et al. 2017, MNRAS, 464, 2396; Loyd & France 2014, ApJS, 211, 9; Luger & Barnes 2015, AsBio, 15, 119; Lundkvist et al. 2016, NatCo, 7, 11201; Mansfield et al. 2018, ApJL, 868, L34; Mazeh et al. 2016, A&A, 589, A75; Murray-Clay et al. 2009, ApJ, 693, 23; Newton et al. 2019, ApJL, in press (arXiv:1906.10703); Noack et al. 2017, SSRv, 212, 877; Nortmann et al. 2018, Science, 362, 1388; Oklopcic 2019, ApJ, submitted (arXiv:1903.02576); Oklopcic & Hirata 2018, ApJL, 855, L11; Owen & Lai 2018, MNRAS, 479, 5012; Owen & Wu 2016, ApJ, 817, 107; Owen & Wu 2017, ApJ, 847, 29; Pallavicini et al. 1981, ApJ, 248, 279; Pizzolato et al 2003, A&A, 397, 147; Ribas et al. 2005, ApJ, 622, 680; Ribas et al. 2016, A&A, 596, A111; Salz et al. 2018, A&A, 620, A97; Sanz-Forcada et al. 2011, A&A, 532, A6; Schneiter et al. 2007, ApJL, 671, L57; Seager & Sasselov 2000, ApJ, 537, 916; Shaikhislamov et al. 2018, MNRAS, 481, 5315; Skumanich 1972, ApJ, 171, 565; Spake et al. 2018, Nature, 557, 68; Tu et al. 2015, A&A, 577, L3; van Eylen et al. 2018, MNRAS, 479, 4786; Vidal-Madjar et al. 2003, Nature, 422, 143; Yan & Henning 2018, Nature Astronomy, 2, 714; Yelle 2004, Icarus, 170, 167

The Need for Exoplanet Masses to Contextualize Atmospheric Characterization Efforts

Background

A tension exists between the desire to expeditiously study the atmospheres of *TESS*-discovered exoplanets with *HST* and the goal of carefully vetting and selecting the optimal set of planets for such studies. Haste is needed to capitalize on the limited and unknown remaining lifetime of *HST* and to prepare for the impending start of the *JWST* mission. However, care is also required to select targets that will provide unambiguous scientific returns. For this reason, a certain amount of pre-vetting of each planet candidate is necessary before the valued eyes of *HST* should be trained on it. In this white paper, we focus on the need for precise mass determinations of *TESS*-discovered exoplanets prior to *HST* observations.

The Need for Masses

A planet's mass is its primary defining characteristic, yet measuring the masses of the multitude of exoplanet candidates found via transit surveys is the main bottleneck to confirming them as true planets. Knowledge of a planet's mass in turn informs our expectation of its atmospheric composition — we would expect a small dense planet to have a very different atmosphere from one that is large and low-density.

Without prior knowledge of a planet's mass, degenerate interpretations of atmospheric spectra are likely. For example, for transmission spectra a strong degeneracy exists between the atmospheric temperature (T), mean molecular weight (μ), and surface gravity (g), which each factor into setting the planet's scale height ($H = \frac{kT}{\mu g}$) and in turn the depth of its spectral features. This degeneracy is especially problematic for small planets, whose atmospheres are not presumed to be hydrogen-rich and can have plausible mean molecular weight values that span over an order of magnitude. We have previously shown the negative effects of unknown planetary mass on interpreting transmission spectra (Batalha, Kempton, & Mbarek, 2017; and see Figure 1), and comparable degeneracies are likely to crop up for emission spectra as well. We therefore caution that in many cases it is unwise to propose for atmospheric characterization observations with *HST* or other facilities without first obtaining mass constraints for the target of interest.

How Precisely Must the Planet's Mass be Known?

Obtaining ground-based RV mass measurements is both time and resource intensive. We therefore seek to provide advice on the precision to which a planet's mass should be measured, such that it is not the limiting factor in determining atmospheric properties. We address this question by performing retrievals on simulated transmission spectra, assuming different degrees of uncertainty on the planet's mass.

We show an example of these calculations in Figure 2. For a *TESS*-like rocky exoplanet orbiting an M 4.5 star, we find that uncertainties in the planet's mass beyond the 50% level begin to substantially degrade the fidelity of a retrieval on its atmospheric composition. On

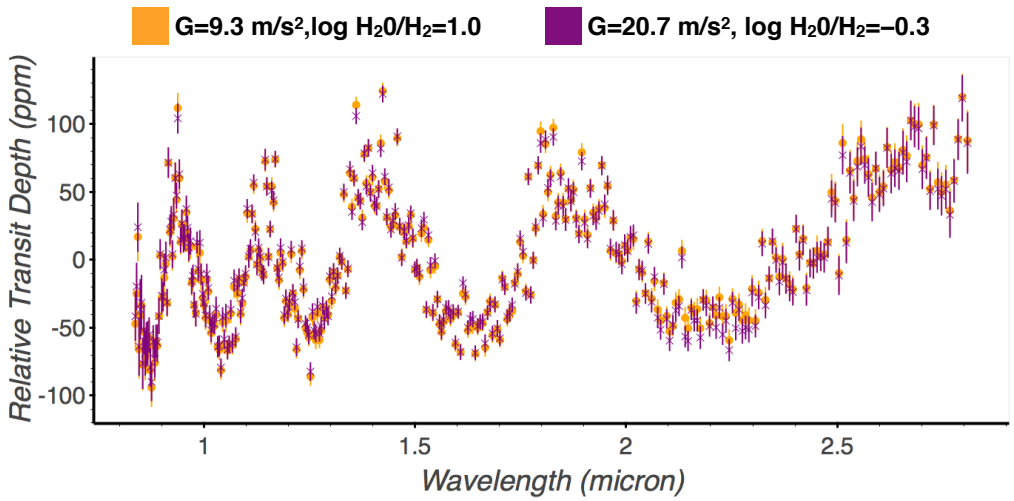

FIGURE 1. An example of how unknown planetary mass leads to a degenerate interpretation of transmission spectra. The planet modeled here has a radius of 1.5 $R_\oplus$ and orbits an M 4.5 star. The spectrum shown in yellow for a surface gravity of 9.3 m s^{-2} and a high water abundance is statistically indistinguishable from the one shown in purple for a surface gravity of 20.7 m s^{-2} and a low water abundance. The former is consistent with a bulk water-rich planet, while the latter is consistent with a rocky planet possessing a hydrogen-rich atmosphere. Only measurements of the planet's mass can break this degeneracy. (Figure adapted from Batalha, Kempton, & Mbarek, 2017.)

the other hand, increasing the precision in the planet's mass to better than 50% results in only minor improvements in the retrieval of atmospheric abundances. Based on this simulation and others that we have run on a sample of sub-Neptunes and super-Earths (Batalha et al., in prep.), we therefore suggest a 50% rule of thumb for the precision of exoplanet mass measurements prior to undertaking atmospheric characterization.

In addition to the negative consequences on retrieved parameters, it is also challenging to assess reasonable *priors* on atmospheric composition if the planet's mass, and therefore its bulk density, is unknown at the outset. This in turn makes it difficult to plan an appropriate set of *HST* observations to return scientifically meaningful results. We stress again that the primary source of uncertainty on atmospheric priors is removed if the planet's mass is known.

Recommendations for Proposal Evaluation

We recommend caution in selecting planets lacking measured masses for atmospheric characterization observations with *HST*. For cases in which a clear path toward precisely measuring a target's mass is put forth, the TAC should still proceed with care. Use of an empirical mass-radius relation (e.g. Chen & Kipping 2017) to predict a likely planetary mass and to guide predictions for atmospheric characterization is insufficient. For any given planetary size, a range of possible masses exist, and both the expected signal amplitude and atmospheric interpretation can depend substantially on which end of that range the planet's mass ultimately falls on.

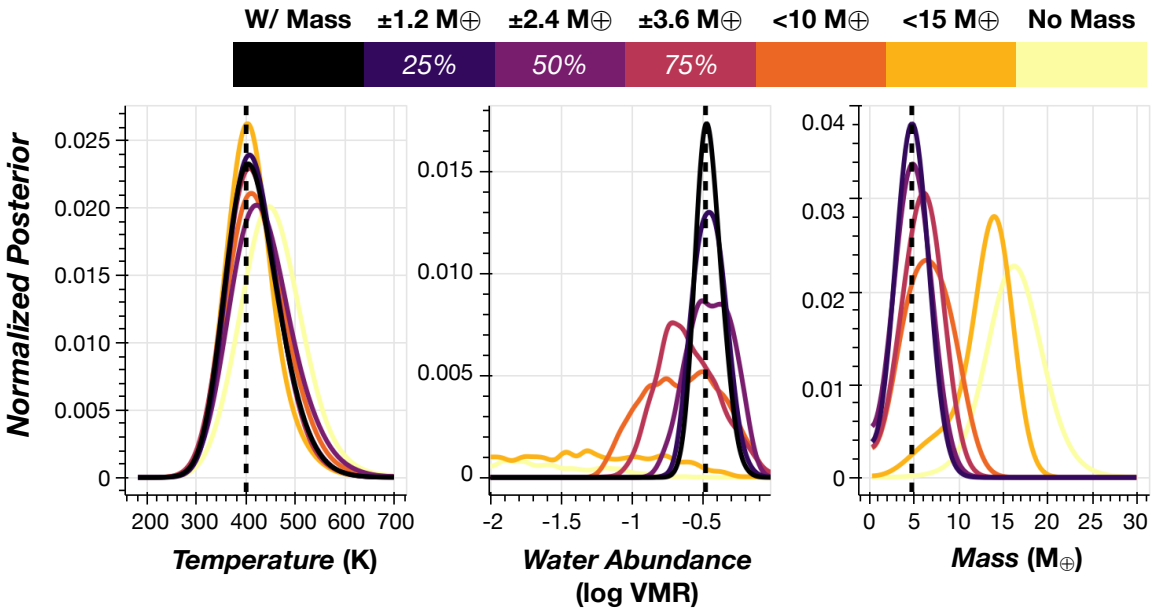

FIGURE 2. Posterior distributions for retrievals on an example *TESS*-like planet with its mass known to varying degrees of uncertainty (as indicated by the color bar at top). The planet modeled here is the same one shown in Figure 1, for the 20.7 m s^{-2} surface gravity case (M_p = 4.75 $M_\oplus$, R_p = 1.5 $R_\oplus$). We find that uncertainties in the planet's mass greater than 50% fundamentally limit the ability to retrieve accurate atmospheric parameters. While the results shown here are for simulated observations with *JWST* NIRSpec, we find comparable results for *HST* spectroscopy as well (Batalha et al., in prep.).

The onus is on the proposers to justify their request for *HST* time for planets lacking precise mass measurements. At minimum, this should include signal-to-noise calculations and a thorough explanation for what will be learned from the proposed observations if the planet's mass lands at either of the far ends of the plausible mass range. The proposers should also present the timeline for RV mass measurements for their chosen target(s), including a worst-case scenario if the planet's mass turns out to be smaller than what is nominally expected. As seen from our analysis presented above, a maximum of 50% uncertainty on an exoplanet's mass should be seen as the threshold at which atmospheric characterization uncertainties are not dominated by the planet's unknown mass.

Our goal in placing such stringent recommendations for which *TESS* candidates should be selected as *HST* targets is not intended to limit, but rather enable excellent science with *HST*. In some cases, waiting an extra cycle to propose observations for a specific target will provide the necessary context to make those observations successful. RV observations are time consuming but do not need to be the limiting factor on high-quality exoplanet science coming out of *HST*. The *TESS* Follow-up Obseving Program (TFOP) is well-organized and able to quickly coordinate RV campaigns on objects of interest as they are discovered. The ideas set forth in this white paper may be used as extra motivation for the TFOP to prioritize mass measurements of exoplanets that will be high-quality observational targets for *HST* and *JWST*.

References:

Batalha, N. E., Kempton, E. M.-R. & Mbarek, R. 2017, ApJ, 836, L5
Chen, J., & Kipping, D. 2017, ApJ, 834, 17

Detecting volcanically produced tori along orbits of exoplanets using UV spectroscopy

1. Introduction

Significant progress has been made since the discovery of the first exoplanet, 51 Peg b (Mayor & Queloz, 1995), including collecting statistics on occurrence rates, masses, and radii of exoplanets (www.exoplanet.eu). Characterization is the next logical step. The Hubble Space Telescope (*HST*) is providing crucial observations for planet atmospheric characterization, particularly at ultraviolet (UV) wavelengths, which are not accessible from the ground.

HST has been extremely effective in characterizing the upper atmospheres of giant exoplanets by observing escaping hydrogen (e.g., Vidal-Madjar et al., 2003; Ehrenreich et al., 2015; Bourrier et al., 2018) and minor species present in the upper atmospheres of these planets (Fossati et al., 2010; Haswell et al., 2012; Vidal-Madjar et al., 2013). Characterizing the atmospheres of small rocky planets is more difficult due to their smaller sizes and pressure scale heights compared to those of giant planets. We suggest a new method for characterizing rocky exoplanets, namely, the detection of volcanically-produced tori lying along the planetary orbits. As we show below, *HST* is capable of detecting an Io-like plasma torus around a bright M dwarf in the solar neighborhood. Observations of this kind would be extremely timely as they would combine the unique observational capabilities of *HST*, particularly at far-UV (FUV) wavelengths, and new targets discovered by the *TESS* satellite. *TESS* is a whole-sky survey (Ricker et al., 2016) that is currently detecting a number of planets orbiting bright (V<10 mag) and close enough (<50 pc) systems to enable characterization. Because of the large number of M dwarfs in the solar neighborhood and the red bandpass and observing windows of *TESS*, one can expect that *TESS* is likely to detect numerous close-in planets orbiting M dwarfs (Barclay et al., 2018). Follow-up *HST* observations of these systems, particularly at FUV wavelengths, will give us important insights into atmospheres and even interior compositions of these planets.

2. Status of research

An exoplanet requires internal heating sources to drive its volcanic activity. Several sources of internal energy are known for planets: radioactive decay, mantle differentiation, (inner) core formation, tidal heating, and induction heating. Due to the compactness of the planetary systems so far detected orbiting late M dwarfs and to the strong magnetic fields of the host stars, the latter two mechanisms, while insignificant for the Earth, can be very powerful for planets orbiting M dwarfs. Both of them are capable of generating enough heat to produce a global subsurface magma ocean (Kislyakova et al., 2017; Dobos et al., 2019).

A sub-surface magma ocean can drive enormous volcanic activity, as is the case for the Jovian satellite Io due to the tidal interaction with other Galilean satellites (Peale et al., 1979). Outgassed material is quickly lost to space, and forms a torus around Jupiter, along the moon's orbit, populated mostly by oxygen and sulfur atoms and ions (Fig. 1; e.g.,

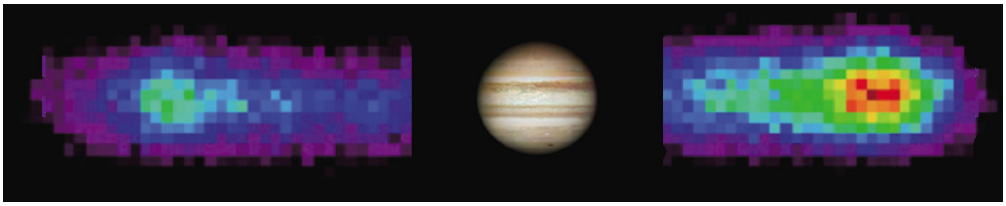

FIGURE 1. Observation of the Io plasma torus in SIII line by *Hisaki* satellite (Murakami et al., 2016).

Murakami et al., 2016). Io's torus has been observed both from space by the UVIS instrument on-board Cassini (Steffl et al., 2004) and by Voyager 1 (Volwerk, 2018), and from the ground (e.g., Thomas, 1996). Techniques for the removal of the geocoronal emission produced by neutral hydrogen and oxygen have been only recently developed (Ben-Jaffel & Ballester, 2013), which is probably why Io's torus has not yet been observed with *HST*.

We suggest that similar tori can be produced by exoplanets in close orbit around late M dwarfs. A dense-enough torus can absorb the stellar light at the position of strong resonance lines of abundant elements, as in the case of the WASP-12 system (Haswell et al., 2012; Fossati et al., 2013). Kislyakova et al. (2018) studied the detectability of absorption signatures by OI superposed to the stellar FUV emission triplet at $\lambda \approx 1304$ Å taking the HST/STIS E140M observations of the active M dwarf AD Leo as a reference for the line strength and width. They have shown that at a spectral resolution of about 50 000 (e.g., HST/STIS E140M grating) and a signal-to-noise ratio (S/N) of 10, which is currently reachable with *HST* for nearby M dwarfs, the torus would be detectable during one *HST* orbit if it had a column density larger than 10^{13} cm^{-2} (Fig. 2). For comparison, the column density of Io's torus is of the order of 10^{13}–10^{14} cm^{-2} (Steffl et al., 2004). Planets orbiting M dwarfs are likely subject to efficient atmospheric escape (e.g., Airapetian et al., 2017; Garcia-Sage et al., 2017), which makes formation of an even denser plasma torus likely. Previously, Demory et al. (2016) have found indications of volcanism on 55 Cnc e by observing secondary eclipses and phase curves at mid-infrared wavelengths. Ridden-Harper et al. (2016) have detected a tentative sodium signal for 55 Cnc e, which could potentially also have origin in volcanic activity. These studies suggest that volcanism can in principle be detectable on exoplanets.

HST follow-up observations of planets orbiting M dwarfs can be used for detection of volcanic activity on these planets. Both tidal and induction heating are the most effective in planets orbiting late-type M dwarfs, due to compactness of these systems and very strong stellar magnetic fields (e.g. Shulyak et al., 2019). However, these stars are also very dim, which requires very long integration times for observations. We suggest to focus on rocky planets orbiting M dwarfs of spectral types M4–M5, as they are still sufficiently bright, but also still likely to have planets with a sub-surface magma ocean due to tidal or induction heating. A possible target already available is the TRAPPIST-1 system. TTVs that are detected are indicative of tidal effects, including heating (Luger et al., 2017). This system has been observed by the *HST* (de Wit et al., 2018), however, one needs a brighter star to allow for the characterization of a torus. Therefore, a bigger and hotter star of a spectral class M4-M5 with a close-in rocky planet would be an ideal target. Observations of such tori have never been attempted before as only recently *TESS* has given us the possibility to find adequate targets for these novel observations.

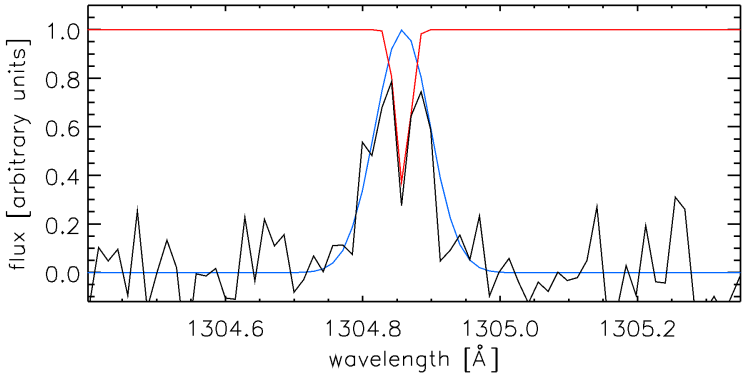

FIGURE 2. Synthetic Gaussian profile of the OI line at 1304.858 Å (blue) superposed to a synthetic Voigt absorption feature (red) computed assuming a column density of $10^{13}\,\mathrm{cm}^{-2}$. The final emission line (black), which includes the torus absorption, was computed assuming a signal-to-noise ratio of 10. The spectral resolution is that of the E140M HST/STIS grating. From Kislyakova et al. (2018).

3. SCIENCE GOALS OF A POSSIBLE UV OBSERVATIONAL STUDY

Planet atmospheric composition and escape - detecting a torus along the orbit will help us constraining the intensity of escape processes for planets orbiting M dwarfs. The torus will also enable us to identify the main constituents of the atmosphere.

Detection of exoplanet volcanic activity - detecting a plasma torus would confirm the presence of active volcanoes on exoplanets. The material forming the torus should be constantly replenished by outgassing from the planetary interior, which in turn is supplied by the planet's volcanic activity.

Characterization of planetary interiors - *HST* observations of the torus will uniquely enable us to constrain the internal composition of exoplanets. This is because the composition of the outgassed material is directly connected to the composition and redox state of the planetary mantle (Gaillard & Scaillet, 2014). Therefore, observations of this kind would give us the unique opportunity to reveal key properties of planetary interiors, which would be difficult or even impossible to obtain in any other way.

4. CONCLUSIONS

The *TESS* mission is going to play a pivotal instrumental role in our future understanding of planets, particularly by providing numerous low-mass, transiting planets in close orbit to bright and nearby stars. Ultraviolet observations conducted with *HST* have successfully demonstrated their capability of detecting atomic and ionic species escaping from the atmospheres of giant planets. Furthermore, realistic predictions indicate that the same is going to be possible also for the tori of rocky planets in close orbit to nearby M dwarfs. *HST*'s remaining operational time is limited and it is of crucial importance to make best use of its capabilities, particularly at UV wavelengths, to gain as much observational material as possible to inform the science and guide the requirements of the next generation of space telescopes with UV capability.

References

Airapetian, V. S., Glocer, A., Khazanov, G. V., et al. 2017, ApJ, 836, L3
Barclay, T., Pepper, J., & Quintana, E. V. 2018, ApJS, 239, 2
Ben-Jaffel, L., & Ballester, G. E. 2013, A&A, 553, A52
Bourrier, V., Lecavelier des Etangs, A., Ehrenreich, D., et al. 2018, A&A, 620, A147
de Wit, J., Wakeford, H. R., Lewis, N. K., et al. 2018, Nature Astronomy, 2, 214
Demory, B.-O., Gillon, M., Madhusudhan, N., & Queloz, D. 2016, MNRAS, 455, 2018
Dobos, V., Barr, A. C., & Kiss, L. L. 2019, A&A, 624, A2
Ehrenreich, D., Bourrier, V., Wheatley, P. J., et al. 2015, Nature, 522, 459
Fossati, L., Ayres, T. R., Haswell, C. A., et al. 2013, ApJ, 766, L20
Fossati, L., Haswell, C. A., Froning, C. S., et al. 2010, ApJ, 714, L222
Gaillard, F., & Scaillet, B. 2014, Earth and Planetary Science Letters, 403, 307
Garcia-Sage, K., Glocer, A., Drake, J. J., Gronoff, G., & Cohen, O. 2017, ApJ, 844, L13
Haswell, C. A., Fossati, L., Ayres, T., et al. 2012, ApJ, 760, 79
Kislyakova, K. G., Fossati, L., Johnstone, C. P., et al. 2018, ApJ, 858, 105
Kislyakova, K. G., Noack, L., Johnstone, C. P., et al. 2017, Nature Astronomy, 1, 878
Luger, R., Sestovic, M., Kruse, E., et al. 2017, Nature Astronomy, 1, 0129
Mayor, M., & Queloz, D. 1995, Nature, 378, 355
Murakami, G., Yoshioka, K., Yamazaki, A., et al. 2016, Geophys. Res. Lett., 43, 12,308
Peale, S. J., Cassen, P., & Reynolds, R. T. 1979, Science, 203, 892
Ricker, G. R., Vanderspek, R., Winn, J., et al. 2016, in Proc. SPIE, Vol. 9904, Space Telescopes and Instrumentation 2016: Optical, Infrared, and Millimeter Wave, 99042B
Ridden-Harper, A. R., Snellen, I. A. G., Keller, C. U., et al. 2016, A&A, 593, A129
Shulyak, D., Reiners, A., Nagel, E., et al. 2019, arXiv e-prints, arXiv:1904.12762
Steffl, A. J., Stewart, A. I. F., & Bagenal, F. 2004, Icarus, 172, 78
Thomas, N. 1996, A&A, 313, 306
Vidal-Madjar, A., Lecavelier des Etangs, A., Désert, J. M., et al. 2003, Nature, 422, 143
Vidal-Madjar, A., Huitson, C. M., Bourrier, V., et al. 2013, A&A, 560, A54
Volwerk, M. 2018, Ann. Geophys., 36, 831